Sustainable Energy & Fuels

PAPER

View Article Online
View Journal | View Issue

Cite this: *Sustainable Energy Fuels*, 2019, **3**, 1388

Suppressing the formation of NO_x and N_2O in CO_2/N_2 dielectric barrier discharge plasma by adding CH_4: scavenger chemistry at work†

Ramses Snoeckx, *[ab] Karen Van Wesenbeeck,[c] Silvia Lenaerts,[c] Min Suk Cha[a] and Annemie Bogaerts[b]

The need for carbon negative technologies led to the development of a wide array of novel CO_2 conversion techniques. Most of them either rely on high temperatures or generate highly reactive O species, which can lead to the undesirable formation of NO_x and N_2O when the CO_2 feeds contain N_2. Here, we show that, for plasma-based CO_2 conversion, adding a hydrogen source, as a chemical oxygen scavenger, can suppress their formation, *in situ*. This allows the use of low-cost N_2 containing (industrial and direct air capture) feeds, rather than expensive purified CO_2. To demonstrate this, we add CH_4 to a dielectric barrier discharge plasma used for converting impure CO_2. We find that when adding a stoichiometric amount of CH_4, 82% less NO_2 and 51% less NO are formed. An even higher reduction (96 and 63%) can be obtained when doubling this amount. However, in that case the excess radicals promote the formation of by-products, such as HCN, NH_3 and CH_3OH. Thus, we believe that by using an appropriate amount of chemical scavengers, we can use impure CO_2 feeds, which would bring us closer to 'real world' conditions and implementation.

Received 29th November 2018
Accepted 17th February 2019

DOI: 10.1039/c8se00584b

rsc.li/sustainable-energy

1. Introduction

The global challenge of climate change and the need for carbon negative technologies have sparked research interest in a wide variety of techniques capable of converting CO_2.[1–6] This CO_2 can be captured either from major emission sources or—preferably, in the long run— from air, through direct air capture (DAC).[7] Numerous analyses and comparisons between different technologies have been made in the literature; however, they all overlook a key aspect that has major consequences, *i.e.* the fact that lab-scale studies generally use pure gases (99.999% purity), whereas industrial gases (with some exceptions) usually contain N_2. Purification is one option, but an energy intensive, and thus costly one.[8] Another—more practical—option is to directly use these impure gases.

However, this option comes with an important obstacle. Most novel technologies under consideration for the conversion of CO_2 into CO and O_2 either require high temperatures (*e.g.*, solar thermochemical and catalytic thermochemical conversion) or create highly reactive O species *in situ* (*e.g.*, electrochemical, photochemical and plasmachemical conversion).[1] As a result, the risk of producing nitrogen oxides (NO_x) and nitrous oxide (N_2O) is real.[9,10] In combustion science, the formation of NO_x and N_2O is a well-understood phenomenon.[11,12] Among the three major NO_x formation mechanisms (*i.e.*, thermal NO_x (Zel'dovich), prompt NO_x, and fuel NO_x), the thermal mechanism consistently produces NO_x, as long as O_2 and N_2 coexist under high temperature conditions (>1900 K).[11] N_2O, on the other hand, is not a major by-product in combustion processes, except for fluidized bed combustion.[12] When released in the atmosphere, these compounds lead to severe air pollution, such as smog and acid rain, and they are responsible for the formation of tropospheric ozone.[13] With respect to global warming, the production of N_2O, in any CO_2 conversion process, cancels out the carbon negative effect of any CO_2 converted, since N_2O is 298 times more potent as a greenhouse gas.[13] This is why NO_x and N_2O emissions are so strictly regulated worldwide.

Despite the potential risk of producing unwanted NO_x and N_2O during the conversion of impure CO_2 feeds containing N_2, almost no research has been performed in this area, for the novel technologies that are being considered to convert CO_2. It stands, without doubt, that this is an important issue, as additional deNO_x post-treatment, or more severe CO_2 pre-purification steps, will have a negative effect on the energy and cost balance of these CO_2 conversion technologies. In previous studies, we reported that, for non-thermal plasma technology—one of the most promising technologies for the conversion of

[a]*King Abdullah University of Science and Technology (KAUST), Clean Combustion Research Center (CCRC), Physical Science and Engineering Division (PSE), Thuwal 23955, Saudi Arabia. E-mail: Ramses.snoeckx@kaust.edu.sa*

[b]*Research Group PLASMANT, Department of Chemistry, University of Antwerp, Universiteitsplein 1, BE-2610 Antwerp, Belgium*

[c]*Research Group DuEL, Department of Bioscience Engineering, University of Antwerp, Antwerp, Belgium*

† Electronic supplementary information (ESI) available. See DOI: 10.1039/c8se00584b

CO_2 (ref. 1)—the presence of N_2 indeed causes the aforementioned formation of NO_x and N_2O.[9,10]

Here, we explore a potential solution to prevent the formation of NO_x and N_2O, *in situ*, during the plasmachemical conversion of CO_2. A well-known solution from combustion science has been the addition of more fuel (eq. to a higher fuel-to-air ratio).[13] Despite the fact that we work under experimental conditions that are very different from those in combustion science, we can justify using a similar approach, based on the results obtained in our previous studies.[9,14,15] We already know that the addition of a hydrogen source to non-thermal pure CO_2 plasmas can trap free O species, *in situ*.[14] And exactly these free O species are responsible for the NO_x and N_2O production pathways in non-thermal plasmas.[9] Therefore, here we introduce the use of a hydrogen source, CH_4, as a chemical oxygen scavenger to suppress the formation of NO_x and N_2O, *in situ*, during the conversion of CO_2 mixtures containing N_2, in a dielectric barrier discharge (DBD) plasma.

2. Materials and methods

Experiments were carried out in a coaxial DBD plasma reactor operating at room temperature and atmospheric pressure. A stainless steel mesh (high voltage electrode) was wrapped over the outside of a quartz tube, and a stainless steel rod (ground electrode) was placed at its centre. Feed gases were composed of CO_2, N_2 and CH_4 (Air Liquide, Alphagaz 1, 99.999%), and each flow rate was controlled using a mass-flow controller (Bronkhorst, EL-Flow select F-210CV). The DBD reactor was powered by an AC high-voltage power supply (AFS, custom made), and the applied voltage and electrical current were sampled using a four-channel digital oscilloscope (Picotech, PicoScope 64201). Finally, Fourier transform infrared spectroscopy (FTIR; Thermo Fischer Scientific, Nicolet 380) was used to study the effects of the addition of CH_4 on the formation of N_2O and NO_x compounds (*i.e.*, NO, NO_2, N_2O_3 and N_2O_5). A detailed description of the set-up and experimental conditions can be found in Section 1 of the ESI.†

2.1. CH_4 as a chemical oxygen scavenger to suppress NO_x production

Despite the many advantages offered by plasma technology for the conversion of CO_2, two main challenges remain:[1]

(1) Separation: the output of a plasma reactor consists of a homogeneous gas mixture; in the case of plasma-based CO_2 conversion, it yields a mixture of CO and O_2 (and any unreacted CO_2) that is very difficult (and thus energy-intensive) to separate by conventional methods;

(2) Impurities: the presence of other gases (even those generally considered to be chemically inert) influences both the physical properties of the plasma and its chemistry; in the case of plasma-based CO_2 conversion, the presence of N_2 results in the undesired formation of NO_x and N_2O.

Here, we show how focussing on the plasma chemistry can help us to simultaneously find answers to both the separation and impurity issues, in the case of a DBD plasma reactor used for the conversion of an impure CO_2 feed containing N_2.

As a baseline case, we studied a DBD operating at a specific energy input (SEI) of 12 kJ L^{-1}, for a 1 : 1 mixture of CO_2 : N_2. Detailed experimental and modelling results for a wide variety of CO_2 : N_2 mixing ratios were discussed in a previous study,[9] with the highest NO_x production occurring for the 1 : 1 case, which is the main reason why we chose to further explore that condition first. A chemical analysis revealed that NO_x species are formed through several pathways in the presence of N_2, during plasma processing of CO_2. The main formation mechanism, for all the different NO_x species, starts with a reaction involving O (or O_2) and N (or $N_2(A^3)$) (see also Section 2.2 below).[9] This observation is complementary with that made in a previous study, which showed that it was possible to chemically trap oxygen species, *in situ*, by adding a hydrogen source.[14] Additionally, another separate study showed that when O and H radicals are present in a plasma, their natural tendency is to form H_2O.[15] Therefore, by combining these three observations, it becomes apparent that we are presented with a 'chemical opportunity'. We hypothesize, based on chemical analyses from these prior studies, that the addition of a small stoichiometric amount of a hydrogen source to a CO_2 : N_2 mixture should be sufficient for trapping the O radicals with H species to form OH and H_2O, before the N species can react with the O species and form NO_x and N_2O (Fig. 1).

To verify the validity of our hypothesis that an effective chemical oxygen scavenger can prevent the formation of NO_x and N_2O, we investigated the effects of using CH_4 as a hydrogen source. Some of the most important plasmachemical reactions leading to the formation of the desired hydrogen radicals are the following electron impact dissociation reactions of CH_4:

$$e^- + CH_4 \rightarrow CH_3 + H + e^- \quad (1)$$

$$e^- + CH_4 \rightarrow CH_2 + H + H + e^- \quad (2)$$

$$e^- + CH_4 \rightarrow CH_2 + H_2 + e^- \quad (3)$$

$$e^- + CH_4 \rightarrow CH + H_2 + H + e^- \quad (4)$$

$$e^- + CH_4 \rightarrow C + H_2 + H_2 + e^- \quad (5)$$

These radicals react further through subsequent electron impact dissociation reactions:

$$e^- + CH_3 \rightarrow CH_2 + H + e^- \quad (6)$$

$$e^- + CH_3 \rightarrow CH + H_2 + e^- \quad (7)$$

$$e^- + CH_2 \rightarrow CH + H + e^- \quad (8)$$

$$e^- + CH \rightarrow C + H + e^- \quad (9)$$

$$e^- + H_2 \rightarrow H + H + e^- \quad (10)$$

The most important electron impact dissociation and excitation reactions with CO_2 and N_2 are:

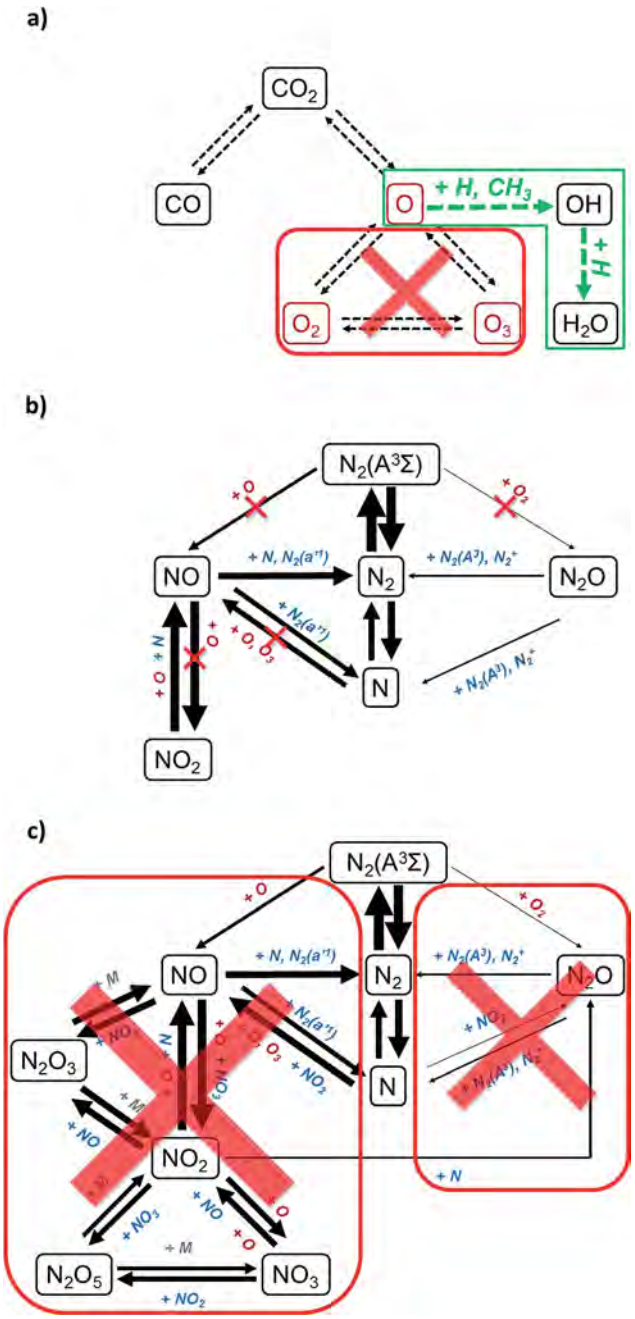

Fig. 1 Simplified reaction scheme illustrating the suppression of the main pathways of the NO_x and N_2O chemistry through the addition of CH_4. Reaction pathways starting from CO_2 show the *in situ* trapping of O by H species (a); initiation of the NO_x chemistry, indicating which pathways are eliminated by the *in situ* trapping of O (b); complete overview of the NO_x and N_2O chemistry to be suppressed by the scavenging of oxygen (c). Original reaction schemes have been adapted from ref. 9.

$$e^- + CO_2 \rightarrow CO + O + e^- \quad (11)$$

$$e^- + N_2 \rightarrow N_2(A^3) + e^- \quad (12)$$

$$e^- + N_2 \rightarrow N + N + e^- \quad (13)$$

For more details on these and other types of plasmachemical (electron impact) reactions refer to the existing literature and databases.[1,9,16–19]

We varied the CH_4 addition from 0.1 up to 2.0 mol% of the total $CO_2 : N_2$ mixture, for a DBD under operating conditions similar to those in the baseline case. It is important to note that the introduction of other components influences the physics of the plasma and its chemistry, especially with a species like CH_4, which results in a cascade of reactive compounds, including H and CH_x radicals. As a result, the electron density and temperature, which affect the conversions, can be altered significantly. Additionally, the conversion of CO_2 can also decrease, due to additional back reactions to CO_2, such as:

$$HCO + O \rightarrow CO_2 + H,$$
$$k = 5.00 \times 10^{-11}\ \text{cm}^3 \text{ per molecule per s at 300 K (ref. 20)} \quad (14)$$

$$OH + CO \rightarrow CO_2 + H,$$
$$k = 1.25 \times 10^{-13}\ \text{cm}^3 \text{ per molecule per s at 300 K (ref. 20)} \quad (15)$$

This effect was observed in a previous study, in which adding 2 mol% CH_4 to pure CO_2 yielded a drop in the relative conversion of CO_2 by ~10%.[14]

In Fig. 2, we can clearly see a decrease of both the NO (1875 cm^{-1}) and NO_2 (1599 cm^{-1}) peaks, when adding CH_4 to the mixture, with the NO peak showing the biggest initial decrease, and the NO_2 peak showing a stronger overall response (see also Fig. 3a). The NO peak decreases by 42% upon adding 0.1 mol% CH_4, by 51% with 1.0 mol%, and by 63% with 2.0 mol% CH_4 added. The NO_2 peak, on the other hand, decreases by 32% upon adding 0.1 mol% CH_4, by 82% with 1.0 mol%, and by 96% with 2.0 mol% CH_4 added.

Due to a complete overlap of the CH_4 peaks, we cannot determine whether the N_2O_3 (1309 cm^{-1}) and/or N_2O_5 (1245 cm^{-1}) peaks decrease, upon addition of CH_4. Nevertheless, this would be a logical consequence, since N_2O_3 and N_2O_5 are secondary reaction products from NO and NO_2 (Fig. 1).

The N_2O (2233 cm^{-1}) peak, on the other hand, seems to increase when more CH_4 is added (Fig. 2). This seems in contrast with a severe reduction of the formation of O_2, which is necessary for the production of N_2O from $N_2(A^3)$ (Fig. 1). Therefore, there are two options: either the N_2O concentration is indeed increasing or its decrease is masked in the FTIR spectra due to interference of other compounds with a similar absorption of the IR frequency (both options are further discussed in Section 2.2).

Besides the decrease in NO and NO_2 peak intensities, some additional peaks started to emerge from the noise when we added 1 mol% CH_4 to the mixture (Fig. 2); they became clearly visible as we increased the CH_4 concentration to 2 mol%. The peak at 3334 cm^{-1} corresponds to HCN;[21] the peak at 1034 cm^{-1} corresponds to CH_3OH;[21] and the peak at 997 cm^{-1} corresponds to NH_3.[21] The HCN peak increases almost linearly, starting from 0.1 mol% CH_4, whereas the CH_3OH and NH_3 peaks only emerge clearly from the noise starting at 1.0 mol% of CH_4 added, and exhibit an exponential increase with further addition of CH_4, to 2 mol% (Fig. 3b).

The formation of these additional components indicates that adding more than 1 mol% CH_4 generates an excess of the

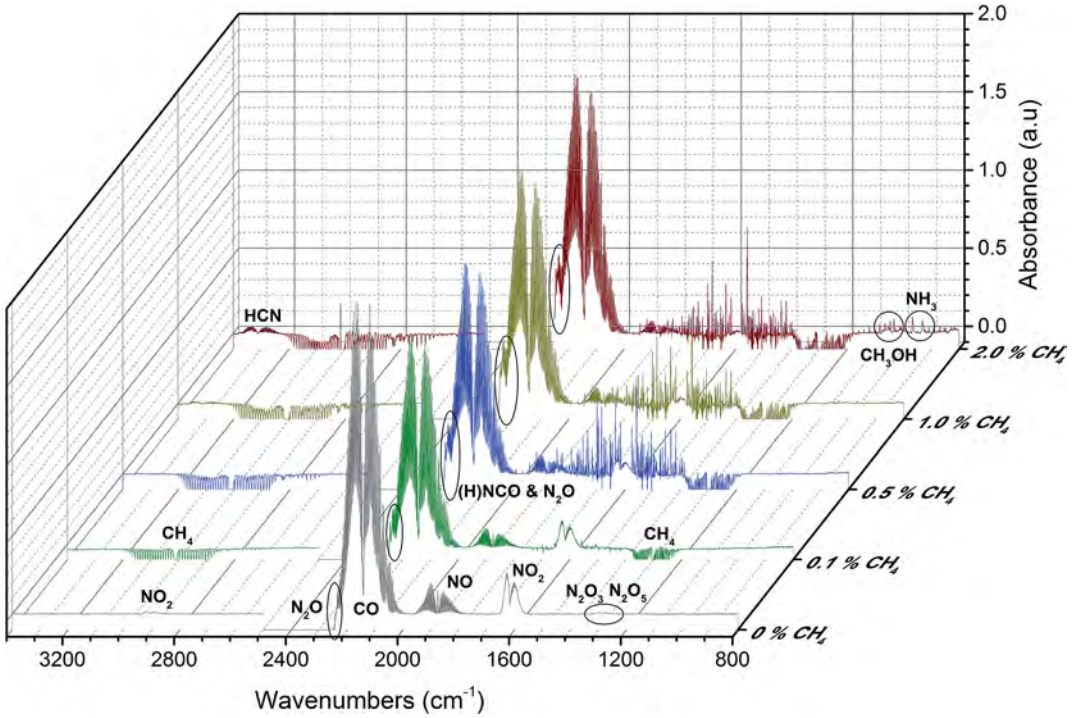

Fig. 2 FTIR spectra of a 1 : 1 mixture of CO_2 : N_2 with 0, 0.1, 0.5, 1.0 and 2.0 mol% CH_4 added. For clarity, the CO_2 peak has been removed. The negative absorbance of the CH_4 bands is due to the subtraction of the blank spectra obtained before turning on the plasma. Original spectra are provided in Section 2.3 of the ESI.†

hydrogen source; most of the O species have been trapped into H_2O and the excess radicals produce some of the typical products that can be expected in a CH_4/N_2 mixture (NH_3 and HCN)[17] and in a CH_4/CO_2 mixture (CH_3OH).[18,22] This result is not surprising and consistent with the stoichiometric balance for adding 1 and 2 mol% CH_4.

By correcting the CO_2 conversion of 3.8% of the baseline case[9] to 3% for the lowered conversion, upon addition of CH_4 (as well as to simplify the balance), and then adding 1 mol% CH_4 (which is almost completely converted, see Table S3 and Fig. S3 in the ESI†), we can construct the following balance:

$$3\%\ CO_2 \rightarrow 3\%\ CO + 3\%\ O \quad (16)$$

$$1\%\ CH_4 \rightarrow 1\%\ C + 4\%\ H \quad (17)$$

$$4\%\ CO + 2\%\ H_2O \quad (18)$$

In this case, the O radicals will readily recombine with the C radicals and form CO, and with the H radicals and form H_2O.

When adding 2 mol% CH_4, (16), (17) and (18) become:

$$3\%\ CO_2 \rightarrow 3\%\ CO + 3\%\ O \quad (19)$$

$$2\%\ CH_4 \rightarrow 2\%\ C + 8\%\ H \quad (20)$$

$$4\%\ CO + 2\%\ H_2O + 1\%\ C + 4\%\ H \quad (21)$$

Hence, besides forming CO and H_2O, the C and H radicals in excess will form other products, such as CH_3OH, HCN, NH_3 and HNCO, as revealed in Fig. 2 and 3. From these stoichiometric balances, it is also clear that the use of CH_4 as a hydrogen source can lead to an increase in CO selectivity. Indeed, when increasing the CH_4 content from 0.1 to 2 mol% the CO peak in the FTIR spectra increases by 42% (see Fig. 2).

In theory the formation of these additional components should not be a major problem, unlike the NO_x formation we are aiming to inhibit, since CH_3OH, HCN and HNCO can be condensed from the CO stream, and for NH_3 efficient scrubbing systems exist.

2.2. Oxygen scavenging chemistry

The experimental results presented in Section 2.1 clearly show that the addition of CH_4 as a chemical oxygen scavenger does indeed suppress the formation of NO_x, *in situ*. The observed trends can be explained by looking at the different reaction rate coefficients of the most important reactions.

Without a hydrogen source, the main components of the mixture are the following: the unreacted CO_2 and N_2, the CO_2 electron impact dissociation products CO and O, and, to a very small extent, the N_2 electron impact dissociation product N and the electron impact excited metastable $N_2(A^3)$. However, due to its high dissociation energy threshold, the conversion of N_2 and thus the concentration of N is very low ($\sim 10^{17}$ cm^{-3}), for a DBD plasma.[9] In addition, although the concentration of $N_2(A^3)$ is higher ($\sim 2 \times 10^{18}$ cm^{-3}), only ~2% ($\sim 4 \times 10^{16}$ cm^{-3}) takes part in the formation of NO_x, due to its fast quenching processes.[9] For these main components, we can establish the following reaction chemistry, which recombines most of the O radicals to form O_2:

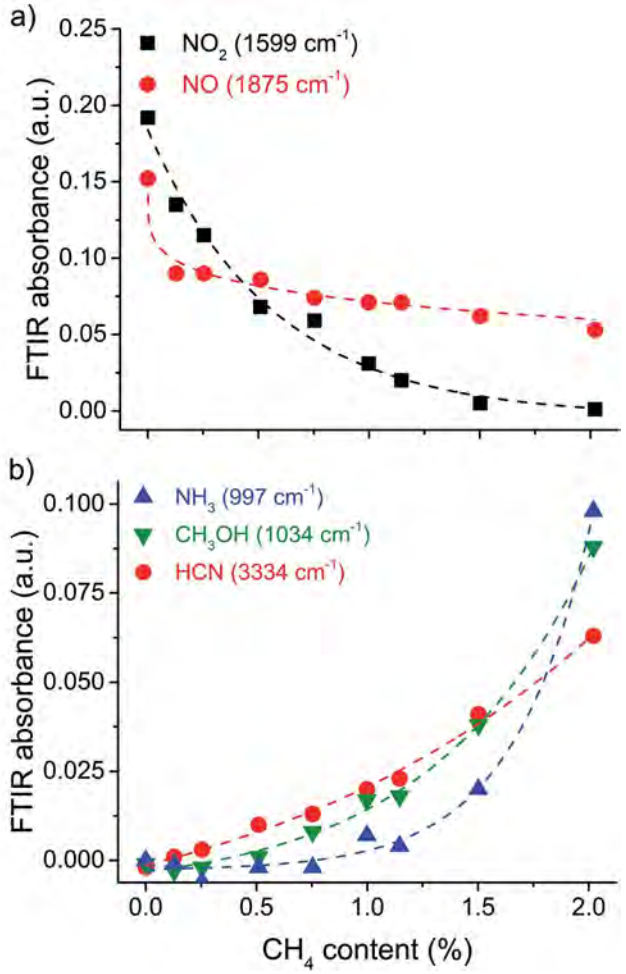

Fig. 3 FTIR absorbance for NO and NO_2 (a); and for NH_3, CH_3OH and HCN (b) as a function of the amount of CH_4 added to a 1 : 1 mixture of CO_2 : N_2 for a SEI of 12 kJ L^{-1}.

$$O + O (+M) \rightarrow O_2 (+M),$$
$k = 1.18 \times 10^{-13}$ cm^3 per molecule per s at 298 K (ref. 23) (22)

However, some of the O radicals, as well as O_3, react with the few N radicals (see Fig. 1):

$$O + N (+M) \rightarrow NO (+M),$$
$k = 2.24 \times 10^{-13}$ cm^3 per molecule per s at 298 K (ref. 23) (23)

$$O_3 + N \rightarrow NO + O_2,$$
$k = 1.00 \times 10^{-16}$ cm^3 per molecule per s at 300 K (ref. 24) (24)

Subsequently, some of the O radicals react with the formed NO:

$$O + NO \rightarrow NO_2,$$
$k = 2.42 \times 10^{-12}$ cm^3 per molecule per s at 300 K (ref. 25) (25)

Additionally, the metastable $N_2(A^3)$ also reacts with the O radicals and O_2:

$$O + N_2(A^3) \rightarrow NO + N,$$
$k = 7.00 \times 10^{-12}$ cm^3 per molecule per s at 300 K (ref. 9) (26)

$$O_2 + N_2(A^3) \rightarrow N_2O + O,$$
$k = 2.00 \times 10^{-14}$ cm^3 per molecule per s at 300 K (ref. 9) (27)

When a small amount (<2 mol%) of CH_4 is added as a hydrogen source, the main components of the mixture are the following: the unreacted CO_2 and N_2 (and to a minor extent CH_4), the CO_2 electron impact dissociation products CO and O, the N_2 electron impact dissociation product N (to a very small extent) and the electron impact excited metastable $N_2(A^3)$, and the CH_4 electron impact dissociation products CH_x and H.[17,18] Up to 0.5 mol% of CH_4 added, the conversion of CH_4 is close to 100%, for 1 mol% of CH_4 added, the conversion is still 89%, but for 2 mol% of CH_4 added, the conversion decreases to 59% (see ESI Table S3 and Fig. S3†). To effectively trap the O radicals and to suppress the formation of NO_x and N_2O, *in situ*, the scavenging reactions need to be faster than reactions 22 to 27 described above. It is important to note that the reaction rate coefficients can only give us an indication of the speed of reaction, so the information presented above needs to be put in perspective. In order to determine the real, exact reaction rates, we would also need to know the densities of all the species and the various chemical equilibria involved. Those can be obtained through the development of a complete and extensive chemical kinetics model.

First, the rate coefficients for O radical scavenging reaction with H and CH_3 radicals (see below) are clearly in the same order and higher than those for the above reactions (22), (23) and (26). Furthermore, the concentrations of H and CH_3 radicals ($\sim 2.5 \times 10^{17}$ to 5×10^{18} cm^{-3}, based on the (nearly) full conversion of CH_4 at 0.1 to 2% CH_4 added) are higher than those of the N radicals ($\sim 10^{17}$ cm^{-3}; see above) and available metastable $N_2(A^3)$ ($\sim 4 \times 10^{16}$ cm^{-3}; see above). Hence, these reactions are estimated to be faster, which means that H and CH_3 radicals are indeed effective chemical oxygen scavengers:

$$O + CH_3 \rightarrow CH_2O + H,$$
$k = 1.40 \times 10^{-10}$ cm^3 per molecule per s at 300 K (ref. 26) (28)

$$O + H (+M) \rightarrow OH (+M),$$
$k = 1.06 \times 10^{-12}$ cm^3 per molecule per s at 300 K (ref. 27) (29)

The CH_2O radical further reacts towards the formation of OH:

$$O + CH_2O \rightarrow HCO + OH,$$
$k = 1.73 \times 10^{-13}$ cm^3 per molecule per s at 300 K (ref. 20) (30)

$$O + HCO \rightarrow CO + OH,$$
$k = 5.00 \times 10^{-11}$ cm^3 per molecule per s at 300 K (ref. 20) (31)

The formed OH radicals get rapidly trapped into H_2O and CH_3OH by subsequent reactions (32)–(35), some of them are even faster than the initial reactions (29)–(31) forming OH. This, in turn, enhances the formation of OH by Le Chatelier's principle, since these reactions rapidly remove the OH radicals from the mixture:

$OH + CH_3 (+M) \rightarrow CH_3OH (+M)$,
$k = 1.00 \times 10^{-10}$ cm^3 per molecule per s at 300 K (ref. 28) (32)

$OH + H (+M) \rightarrow H_2O (+M)$,
$k = 1.65 \times 10^{-11}$ cm^3 per molecule per s at 300 K (ref. 20) (33)

$OH + CH_2O \rightarrow HCO + H_2O$,
$k = 9.37 \times 10^{-12}$ cm^3 per molecule per s at 300 K (ref. 29) (34)

$OH + CH_3 \rightarrow CH_2 + H_2O$,
$k = 1.13 \times 10^{-12}$ cm^3 per molecule per s at 300 K (ref. 28) (35)

In general, all these chemical reactions ((28) to (35)) provide a clear indication of how the addition of CH_4, as an oxygen scavenger, suppresses the formation of NO_x and possibly N_2O. As mentioned above, the increase in the N_2O peak seems contradictory, at first, especially since the formation of O_2 is severely suppressed. One possible explanation could be that the formation of N_2O is effectively suppressed, and its concentration decreases, but this is masked in the FTIR spectra due to interferences from other compounds. Indeed, HNCO (2254–2268 cm^{-1}),[30,31] NCO (2175 cm^{-1})[31] and NCO + OH interactions (2237 cm^{-1})[31] have almost the same FTIR bands as N_2O (2233 cm^{-1}),[21] making it likely that the increased peak in the range 2210–2250 cm^{-1} is the result of an increase of the (H)NCO concentration, which masks the decrease of the N_2O concentration.

Another plausible explanation could be that, although the O_2 formation is suppressed, N_2O is being formed through new different pathways, as a result of the formation of HCN and NH_3. For high temperature conditions, this has been detailed in numerous studies found in the literature describing the combustion chemistry of (de-)NO_x (and fuel NO_x).[11,12] In the next section we analyse whether this chemistry is also relevant for the current low temperature plasma process under study.

2.3. de-NO_x chemistry

Despite scavenging the reactive O species to suppress the NO_x an N_2O formation, the presence of a hydrogen source also leads to a variety of reactants (such as HCN and NH_3), leading, in turn, to the additional formation (or destruction) of NO_x or N_2O. Fig. 4 gives a visual representation of how, at low temperature, a general NO_x reaction scheme of these interactions might look like, for CO_2 : N_2 plasma with the addition of CH_4. It is important to note that this reaction scheme is only of a general character. It is based on the products observed with FTIR and on the most important reactions, defined by their rate coefficients presented in Section 2.4 of the ESI.† To construct an accurate fully supported chemical pathway, it is necessary to build a complete plasma chemical kinetics model that includes a detailed description of the NO_x and by-product chemistry, supported and validated by an extensive quantitative experimental study. For which the current analysis, together with the recent work of Wang *et al.*,[16] can already provide a foundation.

We can summarize the reaction scheme as follows: HCN is formed from reactions of N and NO with CH_x and its concentration increases linearly (Fig. 3b) due to the absence of

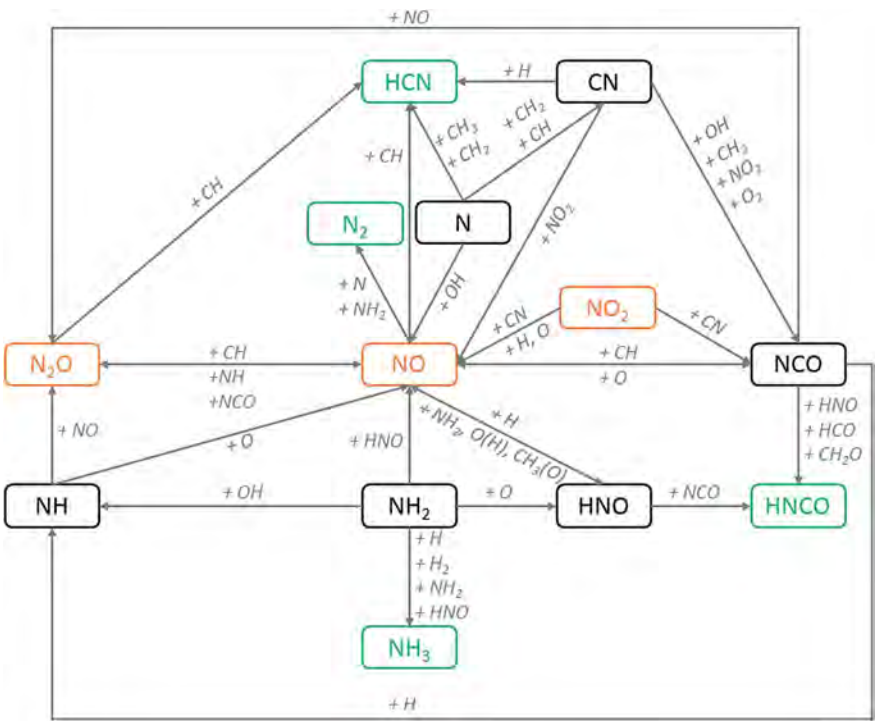

Fig. 4 Basic visual representation of a low temperature NO_x reaction scheme for CO_2 : N_2 plasma with addition of CH_4 (based on the most important reaction rate coefficients presented in Section 2.4 of the ESI†). For double-sided arrows, reactants above the arrows are those for reactions going from right to left, while reactants below the arrows are those for reactions going from left to right. NO_x and N_2O are marked in orange, whereas stable products without important loss processes are marked in green.

important destruction reactions (contrary to what is found in combustion processes). The formation of NH_3, on the other hand, is delayed until an excess of CH_4 is added to the mixture (Fig. 3b), due to the consumption of the NH_x precursors through a reaction with either NO (to form N_2 and N_2O) or O (to form HNO). The formation of CH_3OH is also delayed until an excess of CH_4 is added to the mixture (Fig. 3b), probably due to the consumption of CH_x in the de-NO_x chemistry. Upon addition of CH_4, the NO_2 concentration decreases more than the NO concentration (Fig. 3a) due to the interconversion of NO_2 into NO through reactions with H and O, and due to the formation of NO through several reactions starting from NH_x, HNO and NCO. Nevertheless, the NO concentration continues to decrease, due to destruction reactions with NH_x, CH and H. Finally, N_2O is formed from NO through reactions with NH and NCO, and destroyed by CH, whereas HNCO is formed by reaction of NCO with HCO, HNO and CH_2O, indicating that HNCO is a stable end-product, and that N_2O is converted into HCN as a stable end-product. As a result, the N_2O concentration most likely decreases and the increased peak at 2233 cm^{-1} (Fig. 2) is, in fact, due to the formation of HNCO, rather than an increase in N_2O concentration.

3. Discussion and outlook

We have demonstrated that it is possible to reduce the amount of NO_x produced during plasma-based CO_2 splitting in the presence of N_2 simply by adding a hydrogen source such as CH_4, leading to the almost stoichiometric *in situ* trapping of oxygen. Adding CH_4 at 1 mol% of the total mixture yields NO_2 and NO FTIR absorbance peaks that are 82% and 51% lower than those obtained without the addition of CH_4. Even higher reductions, up to 96% and 63%, are possible when a stoichiometric excess of the hydrogen source is added, which was 2 mol% CH_4 in our case. However, in that case, the excess hydrogen and carbon radicals will lead to the regular plasma-based reforming chemistry, creating several by-products in low concentrations, such as NH_3, HCN, CH_3OH and probably HNCO.

From the data analysis it becomes clear that two processes are responsible for reducing the amount of NO_x produced. The first one is—the process we were aiming for—the direct inhibition of NO_x formation through the fast oxygen scavenging chemistry by the H and CH_x radicals, arising from the introduced CH_4. The second one is the known reduction of NO_x to N_2 in the presence of reducing agents, in this case occurring at room temperature.

These findings suggest that impure CO_2 mixtures containing N_2 may be used as a feedstock, which could have a significant positive impact on the implementation of plasma-based CO_2 conversion research. As a result, there are several interesting follow-up questions. In the present study, we used the most convenient source of hydrogen, CH_4, but it would be interesting to investigate other hydrogen sources.[14] The most fundamental one would be H_2, which could theoretically result in fewer by-products (*cf.* chemical analysis above). However, we could also look into greener and more sustainable hydrogen sources, such as glycerol.[32] From the analysis side, an important challenge to be addressed in future studies is the issue of N_2O and (H)NCO identification. Higher resolution FTIR, or separate N_2O detection using a customized GC (with TCD, ECD, NPD or MS) or custom sensors, might offer a solution.

Additionally, to capture the complete complexity of the underlying mechanisms and to be able to fully analyse and comprehend all the chemical pathways, it will be necessary to build a complete plasma chemical kinetics model with a detailed NO_x and by-product chemistry, supported and validated by a wide range of experiments. A good starting point for the development of such a model would be to expand the NO_x chemistry from Wang *et al.*'s recent work on $CO_2/CH_4/N_2$ mixtures.[16]

It would also be interesting to see whether the same effect can be found for different plasma types, especially for microwave (MW) and gliding arc (GA) plasmas. For these plasmas, the formation of NO_x is much higher, and the dominant pathway proceeds through vibrationally excited N_2 states, rather than through the metastable N_2 state and N radicals.[9,10]

Finally, these results are a clear indication that the plasma chemistry can be controlled to a certain extent by adding small amounts of additives; a similar demonstration has been given by Snoeckx *et al.*[33] in their work on the selective formation of methanol. Despite the seeming trivialness of this insight, directing more research towards simple chemical intervention steps—before turning to complex engineering or plasma-catalysis combinations—could lead to short-term promising advancements in the field of plasma-based CO_2 conversion and hydrocarbon reforming.

Conflicts of interest

There are no conflicts to declare.

Acknowledgements

The research reported in this publication was supported by funding from the "Excellence of Science Program" (Fund for Scientific Research Flanders (FWO): grant no. G0F9618N; EOS ID: 30505023). The authors R. S. and M. S. C. acknowledge financial support from King Abdullah University of Science and Technology (KAUST), under award number BAS/1/1384-01-01.

References

1 R. Snoeckx and A. Bogaerts, *Chem. Soc. Rev.*, 2017, **46**, 5805–5863.
2 M. Mikkelsen, M. Jørgensen and F. C. Krebs, *Energy Environ. Sci.*, 2010, **3**, 43–81.
3 A. Goeppert, M. Czaun, J.-P. Jones, G. K. Surya Prakash and G. A. Olah, *Chem. Soc. Rev.*, 2014, **43**, 7995–8048.
4 P. Lanzafame, G. Centi and S. Perathoner, *Chem. Soc. Rev.*, 2014, **43**, 7562–7580.
5 M. Aresta, A. Dibenedetto and A. Angelini, *Chem. Rev.*, 2014, **114**, 1709–1742.
6 P. Furler, J. R. Scheffe and A. Steinfeld, *Energy Environ. Sci.*, 2012, **5**, 6098–6103.

7 D. W. Keith, *Science*, 2009, **325**, 1654–1655.
8 C. Kolster, E. Mechleri, S. Krevor and N. Mac Dowell, *Int. J. Greenhouse Gas Control*, 2017, **58**, 127–141.
9 R. Snoeckx, S. Heijkers, K. Van Wesenbeeck, S. Lenaerts and A. Bogaerts, *Energy Environ. Sci.*, 2016, **9**, 999–1011.
10 S. Heijkers, R. Snoeckx, T. Kozák, T. Silva, T. Godfroid, N. Britun, R. Snyders and A. Bogaerts, *J. Phys. Chem. C*, 2015, **119**, 12815–12828.
11 J. A. Miller and C. T. Bowmans, *Prog. Energy Combust. Sci.*, 1989, **15**, 287–338.
12 A. N. Hayhurst and A. D. Lawrence, *Prog. Energy Combust. Sci.*, 1992, **18**, 529–552.
13 C. Baird and M. Cann, *Environmental Chemistry*, W. H. Freeman, 4th edn, 2008.
14 R. Aerts, R. Snoeckx and A. Bogaerts, *Plasma Processes Polym.*, 2014, **11**, 985–992.
15 R. Snoeckx, A. Ozkan, F. Reniers and A. Bogaerts, *ChemSusChem*, 2017, **10**, 409–424.
16 W. Wang, R. Snoeckx, X. Zhang, M. S. Cha and A. Bogaerts, *J. Phys. Chem. C*, 2018, **122**, 8704–8723.
17 R. Snoeckx, M. Setareh, R. Aerts, P. Simon, A. Maghari and A. Bogaerts, *Int. J. Hydrogen Energy*, 2013, **38**, 16098–16120.
18 R. Snoeckx, R. Aerts, X. Tu and A. Bogaerts, *J. Phys. Chem. C*, 2013, **117**, 4957–4970.
19 *LXCAT database*, http://www.lxcat.net.
20 D. L. Baulch, C. J. Cobos, R. A. Cox, C. Esser, P. Frank, T. Just, J. A. Kerr, M. J. Pilling, J. Troe, R. W. Walker and J. Warnatz, *J. Phys. Chem. Ref. Data*, 1992, **21**, 411–429.
21 *NIST Chemistry WebBook, NIST Standard Reference Database Number 69*, ed. P. J. Linstrom and W. G. Mallard, National Institute of Standards and Technology, Gaithersburg MD, 2018.
22 R. Snoeckx, A. Rabinovich, D. Dobrynin, A. Bogaerts and A. Fridman, *Plasma Processes Polym.*, 2017, **14**, 1600115.
23 I. M. Campbell and C. N. Gray, *Chem. Phys. Lett.*, 1973, **18**, 607–609.
24 A. J. Barnett, G. Marston and R. P. Wayne, *J. Chem. Soc., Faraday Trans. 2*, 1987, **83**, 1453.
25 R. Atkinson, D. L. Baulch, R. A. Cox, R. F. Hampson, J. A. Kerr, M. J. Rossi and J. Troe, *J. Phys. Chem. Ref. Data*, 1997, **26**, 1329–1499.
26 R. Atkinson, D. L. Baulch, R. A. Cox, R. F. Hampson, J. A. Kerr and J. Troe, *J. Phys. Chem. Ref. Data*, 1992, **21**, 1125–1568.
27 W. Tsang and R. F. Hampson, *J. Phys. Chem. Ref. Data*, 1986, **15**, 1087–1279.
28 D. L. Baulch, C. J. Cobos, R. A. Cox, P. Frank, G. Hayman, T. Just, J. A. Kerr, T. Murrells, M. J. Pilling, J. Troe, R. W. Walker and J. Warnatz, *J. Phys. Chem. Ref. Data*, 1994, **23**, 847–1033.
29 R. Atkinson, D. L. Baulch, R. A. Cox, J. N. Crowley, R. F. Hampson, J. A. Kerr, M. J. Rossi and J. Troe, *Summary of Evaluated Kinetic and Photochemical Data for Atmospheric Chemistry*, 2001.
30 M. S. Lowenthal, R. K. Khanna and M. H. Moore, *Spectrochim. Acta, Part A*, 2002, **58**, 73–78.
31 I. Czekaj, J. Wambach and O. Kröcher, *Int. J. Mol. Sci.*, 2009, **10**, 4310–4329.
32 X. Zhu, T. Hoang, L. L. Lobban and R. G. Mallinson, *Chem. Commun.*, 2009, 2908.
33 R. Snoeckx, W. Wang, X. Zhang, M. S. Cha and A. Bogaerts, *Sci. Rep.*, 2018, **8**, 15929.